538 nm. Broad absorbances also appear at longer wavelength in the 650–700-nm range and in the near-IR. The primary information from these spectra is that the two voltammetric reductions involve spectrally distinguishable species, and so the multiple voltammetric peaks are unlikely to simply arise from morphological swelling heterogeneity within the film.

Acknowledgment. This research was supported in part by grants from the National Science Foundation and the Office of Naval Research.

Registry No. I, 36900-46-6; C, 7440-44-0; Pt, 7440-06-4; $SnCl_2$, 18282-10-5; (1,4,5,8-naphthalenetetracarboxylic acid)(1,2,4,5-tetraaminobenzene) (copolymer), 110851-60-0; 1,4,5,8-naphthalenetetracarboxylic acid, 128-97-2; 1,2,4,5-tetraaminobenzene tetrahydrochloride, 4506-66-5.

References and Notes

(1) (a) *Handbook of Conducting Polymers*; Skotheim, T. A., Ed.; Marcel Dekker: New York, 1986; Vol. 1, 2. (b) Frommer, J. E.; Chance, R. R. *Encyclopedia of Polymer Science and Engineering*, 2nd ed.; Wiley: New York, 1986; Vol. 5, pp 462–507.
(2) (a) Ruan, J. Z.; Litt, M. H. *J. Polym. Sci., Polym. Chem. Ed.* **1987**, *25*, 285. (b) Ruan, J. Z.; Litt, M. H. *Synth. Met.* **1986**, *15*, 237. (c) Iqbal, Z.; Maleysson, C.; Baughman, R. H. *Synth. Met.* **1986**, *15*, 161. (d) Litt, M. H.; Ruan, J. Z. *Polym. Mater. Sci. Eng.* **1986**, *55*, 731. (e) Chien, J. C. W.; Carlini, C. *J. Polym. Sci., Polym. Chem. Ed.* **1985**, *23*, 1383. (f) Bizzarri, P. C.; Della Casa, C. *Mol. Cryst. Liq. Cryst.* **1985**, *118*, 245. (g) Young, C. L.; Whitney, D.; Vistnes, A. I.; Dalton, L. R. *Annu. Rev. Phys. Chem.* **1986**, *37*, 459. (h) Kim, O. K. *J. Polym. Sci., Polym. Lett. Ed.* **1985**, *23*, 137.
(3) (a) Berry, G. C. *J. Poly. Sci., Polym. Symp.* **1978**, *65*, 143. (b) Berry, G. C. *Discuss. Faraday Soc.* **1970**, *49*, 121.
(4) (a) Kim, O. K. *J. Polym. Sci., Polym. Lett. Ed.* **1982**, *20*, 663. (b) Kim, O. K. *Mol. Cryst. Liq. Cryst.* **1984**, *105*, 161.
(5) Polyak, L.; Rolison, D. R.; Kessler, R. J.; Nowak, R. J. 163rd Meeting of the Electrochemical Society; San Francisco, May 8–13, 1983; Extended Abstracts 547, 1983.
(6) Wilbourn, K. O.; Murray, R. W., submitted for publication.
(7) (a) Van Densen, R. L.; Gorns, A. K.; Surei, A. J. *J. Poly. Sci., Polym. Chem. Ed.* **1968**, *6*, 1777. (b) Arnold, F. E.; Van Densen, R. L., *Macromolecules* **1969**, *2*, 497.
(8) Perrin, D. D.; Dempsey, B.; Serjeant, E. P. *pK_a Predictions of Organic Acids and Bases*; Chapman and Hall: London, 1981.
(9) Baizer, M. M.; Lund, H., Eds. *Organic Electrochemistry*; Marcel Dekker: New York, 1983.
(10) (a) MacDiarmid, A. G.; Chaing, J.-C.; Halpern, M.; Huang, W.-S.; Mu, S.-L.; Somasiri, N. L. D.; Wu, W.; Yaniger, S. I. *Mol. Cryst. Liq. Cryst.* **1985**, *121*, 173. (b) MacDiarmid, A. G.; Chang, J. C.: Huang, W. S.; Humphrey, B. D.; Somasiri, N. L. D. *Mol. Cryst. Liq. Cryst.* **1985**, *125*, 309.

Single-Ion Conduction in Poly[(oligo(oxyethylene) methacrylate)-*co*-(alkali-metal methacrylates)]

Eishun Tsuchida,* Norihisa Kobayashi, and Hiroyuki Ohno

Department of Polymer Chemistry, Waseda University, Tokyo 160, Japan.
Received April 9, 1987; Revised Manuscript Received July 1, 1987

ABSTRACT: Thin films of poly[(oligo(oxyethylene) methacrylate)-*co*-(alkali-metal methacrylates)] were prepared from methanol solutions of oligo(oxyethylene) methacrylate and alkali-metal methacrylates by casting and polymerization on a Teflon plate under nitrogen. The ionic conductivity of the films depends on the electrolyte content, the dissociation energy of the alkali-metal methacrylate, and the degree of motion of polymer segments surrounding the ions in the polymer matrix. The ionic conductivity of the polymeric Li and K salts is 10^{-6} S/cm at 80 °C. The transient ionic current after reversing the dc bias polarity shows one sharp peak corresponding to cation migration, indicating that the polymer is a cationic single-ion conductor. The temperature dependence of conductivity was determined. The Williams–Landel–Ferry parameters, calculated from the temperature dependence of conductivity, agreed reasonably well with theoretical values, confirming the influence of polymer segmental motion on conductivity. Additional confirmation was obtained from a Vogel–Tammann–Fulcher plot.

Introduction

Polymeric solid electrolytes with high ionic conductivity are of interest in theoretical and basic research as well as for the development of novel devices. Matrix polymers for such electrolytes include an organic polar polymer/additive system,[1-3] polyether,[4-15] poly(ethylene succinate),[16,17] poly(ethyleneimine),[18] and poly(alkylene sulfide).[19] Combinations of these matrices with $LiClO_4$ show ionic conductivities of 10^{-6}–10^{-9} S/cm at 25 °C. Ionic conductivity as high as 10^{-5} S/cm in the system poly[oligo(oxyethylene) methacrylate]/LiX[13] is attributed to the flexible oligo(oxyethylene) segment, which has a lower glass transition temperature than crystalline poly(oxyethylene). Comblike polymers containing similar oligo(oxyethylene) chains have been used as matrix polymers.[20-23] Shriver et al. report that the hybrid system [polyphosphazene with an oligo(oxyethylene) side chain]/AgO_3SCF_3 has a conductivity of about 10^{-3} S/cm at 70 °C.[20]

However, since these matrices are bi-ion conductors, their ionic conductivities decrease with continued dc voltage even though alkali-metal nonblocking electrodes are used. This problem is attributed to the localization of counteranions near the anode, which inhibits the supply of alkali-metal cations from it. This decrease in dc conductivity prevents the use of such systems in devices driven under dc polarization. Accordingly, a single-ion conductive matrix is required for such uses as dry batteries, sensory systems, and capacitors. Polyelectrolytes should provide such single-ion conductive matrices because the opposite charges are fixed on the polymer chains. However, alkali-metal salts of such polyanions as poly(methacrylic acid) and poly(styrenesulfonic acid) are essentially insulators in the dry state, presumably because their T_g is too high for ionic conduction at ambient temperature and because they contain no segment that promotes salt dissociation. One approach to a single-ion conductor involves blending polyelectrolyte salts with soft segments such as poly(oxyethylene), which renders cations mobile. Selective ion conduction in such blends can be attributed to the relatively larger diffusion constants of small ions compared to those of giant polyions. Another approach involves introduction into a polymer matrix of structural units with

0024-9297/88/2221-0096$01.50/0

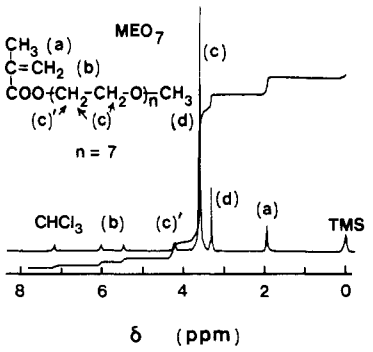

Figure 1. ^{1}H NMR spectrum of MEO_7 monomer in $CDCl_3$ at 25 °C.

larger segmental motion and free volumes. Polyelectrolytes containing high[24] or low[25] molecular weight poly(oxyethylene) are reported to be single-ion conductors.

We here report on copolymers of oligo(oxyethylene) methacrylate with alkali-metal methacrylates as novel polymeric solid electrolytes with a carrier ion source and a low T_g matrix for ionic conduction. This system provides high ionic conduction without additive solvent or inorganic salts. Single-ion ac and dc conductive properties are compared with those of ordinary bi-ion conductors.

Experimental Section

Materials. Alkali-metal methacrylates were prepared by neutralization of a known amount of reagent-grade alkali-metal hydroxide with a large excess of distilled methacrylic acid in dry methanol at 25 °C for 2 h. The solutions were poured into a 10-fold excess of acetone to precipitate the salts (MAM; M = Li, Na, or K). The precipitates were redissolved in methanol and reprecipitated 3 times. They were finally collected on a glass filter, washed several times with dry acetone, and dried in vacuo at 40 °C for 15 h. The absence of free acid was confirmed by IR spectra.[26]

Oligo(oxyethylene) methacrylate (MEO_7, seven oxyethylene units) was prepared and purified as previously described.[13] (See Figure 1 for the ^{1}H NMR spectrum of MEO_7.)

2,2′-Azobis(isobutyronitrile) (AIBN) was recrystallized twice from dry methanol. The dried AIBN was used immediately as the initiator in the free-radical polymerization.

Organic solvents were distilled, stored over 4A molecular sieves, and redistilled before use.

P(MEO_7-*co*-MAM) were prepared as follows. A chloroform solution of MEO_7 was carefully evaporated at room temperature with continuous addition of dry methanol. Given amounts of MAM and AIBN (1 mol % of total vinyl monomers) were added to the methanol solution. The mixture was cast on a Teflon plate and the casting solvent evaporated under dry nitrogen flow over P_2O_5 for 20 h at 80 °C for P(MEO_7–MALi) or 60 °C for P(MEO_7–MANa) and P(MEO_7–MAK). The material remaining on the Teflon plate was then evacuated at 80 °C for 15 h to effect thermal polymerization and complete drying. When P(MEO_7–MAM) films were placed between Li electrodes and kept at room temperature for a week in a dry Ar atmosphere, the metallic luster on the contacted side of the film was retained, suggesting that any moisture in the film had a negligible effect on ionic conduction and that there was no proton conduction.

Methods. All measurements were carried out in a drybox filled with dry Ar. Ionic conductivity measurements were carried out at 1-V ac with a Yokogawa–Hewlett-Packard multifrequency LCR meter Model 4274A over the frequency range 10^2–10^5 Hz. A disk sample, diameter 10 mm, was sandwiched between electrodes of Li or stainless steel. The ac ionic conductivity was calculated from the complex impedance plots[27] with computer curve fitting. The temperature dependence of conductivity was determined by temperature-controlled ac measurement under dry Ar over the range 0–80 °C. Metallic Li or Pt electrodes were used for dc (3 V) conductivity measurements with a Kikusui dc power supply (Model PAC 7-10), a Kikusui millivolt ammeter (Model 115), and a Keithley solid-state electrometer (Model 610C). Details of instrumentation have been described.[13]

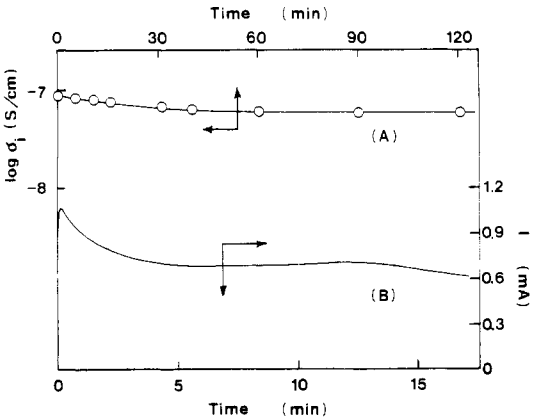

Figure 2. (A) Time dependence of the dc (3 V) ionic conductivity for P(MEO_7–MALi) at 25 °C using metallic lithium electrodes. (B) Transient ionic current for P(MEO_7–MALi) at 80 °C, film thickness 23 μm.

The thermal history of the polymer film was analyzed with a differential scanning calorimeter (SEIKO, Model SSC-580, DSC-10) under dry Ar. Scanning speed was 8 °C/min, and six measurements were made on each sample. The T_g was taken as the temperature of the lower intersection point of the base line with the extrapolated slope in the thermogram.

The X-ray diffraction patterns of the films were determined on an X-ray diffractometer (reflection method, Rigaku Denki Co., Model 2026) with Cu Kα radiation. The film samples were mounted on a glass sample rest, and diffraction patterns were obtained in the 2θ–θ mode. The morphology of the film on the sample rest was also analyzed with a polarizing microscope (SUR-UT, Nikon Co.).

IR spectra were taken with a Japan Spectroscopic Co. Model IR 810 spectrometer, using 1 mg of sample mixed with 70 mg of KBr and pelletized. A NaCl plate was used as a supporing cell for the solute sample.

Results and Discussion

P(MEO_7–MAMs) are insoluble in organic solvents. MEO_7 gelled through solution polymerization in THF solutions >0.5 mol/L at 60 °C. Gelation also occurred during solution polymerization under vacuum at an MEO_7 concentration <0.2 mol/L. Although polymeric MEO_7 [P(MEO_7)] could be obtained as a viscous liquid by homogeneous solution polymerization, it was difficult to prepare thin films by casting a preliminarily polymerized P(MEO_7). Accordingly, we used a polymerization-casting technique to prepare thin films of P(MEO_7–MAM). ^{1}H NMR spectra of methanolic Soxhlet extracts of insoluble P(MEO_7) films indicated that MEO_7 was completely polymerized during polymerization casting. Films prepared by this technique were 100–180 μm thick. These polymeric solid electrolytes showed no endothermic or exothermic change, except for T_g, over the temperature range −150 to 130 °C. An exothermic decomposition occurred above 150 °C.

The dc conductive characteristics of a P(MEO_7–MALi) film were measured on a 10-mm diameter disk sandwiched between Li or Pt electrodes. The time-dependence of the dc conductivity is shown in Figure 2A. Metallic Li electrodes were used as nonblocking electrodes. The dc ionic conductivity of P(MEO_7)/MX hybrid systems decreased by 1–2 orders of magnitude within 60 min, even with nonblocking electrodes. On the other hand, the dc ionic conductivity of P(MEO_7–MALi) films showed excellent stability; since carboxylate ions are covalently bound to the polymer chain and are not mobile under dc polarization, the polymer behaves as a cationic single-ion conductor. In order to assess the single-ion characteristics of

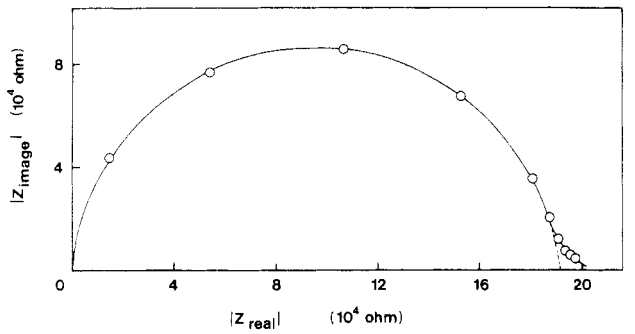

Figure 3. Complex impedance plot for P(MEO_7–MALi) ([Li^+] = 1.68) with metallic lithium electrodes at 25 °C.

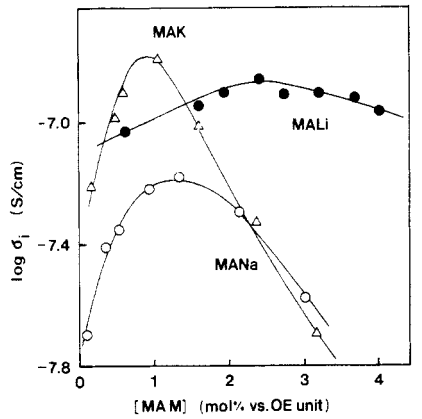

Figure 4. Electrolyte content dependence of the ac (1 V) ionic conductivity for P(MEO_7–MAM).

P(MEO_7–MALi), the transient ionic current of the film was measured (Figure 2B). A bias of 5-V dc was applied to a cell of Pt/P(MEO_7–MALi)/Pt for 10 h at 80 °C, and the bias polarity was then reversed to measure to transient ionic current. Both sharp and broad peaks were observed at 10 s and about 12 min, corresponding to the migration of the cation carrier sheet and the anion contribution, respectively. The carrier mobility was determined from eq 1, where μ = carrier mobility, d = film thickness, V =

$$\mu = d^2/V\tau \qquad (1)$$

applied voltage, and τ = time of maximum current. Strictly, V is a function of time because of the space-charge effect.[28] We used the applied voltage as V in order to calculate the apparent mobilities of the cation (1.0×10^{-7} cm^2 V^{-1} s^{-1}) and anion (1.5×10^{-9} cm^2 V^{-1} s^{-1}). The cation transport number was calculated to be 0.99. Accordingly, the P(MEO_7–MALi) copolymer is a single-ion conductor.

Disk samples of P(MEO_7–MAM) (10-mm diameter) were sandwiched between Li electrodes (for MALi) or stainless steel electrodes (for MANa and MAK) to measure the conductivity with complex impedance plots. These systems were ohmic conductors at applied potentials of 0.5–4.0 V. Subsequent ac measurements were carried out at an electrode potential of 1.0 V. A typical complex impedance plot for P(MEO_7–MALi) is shown in Figure 3. The deviation from the arc in the low-frequency region indicates that the equivalent circuit can be described as the polarization processes in the polymer film and at the electrode interface. The bulk impedance of the film was taken as the intersection of the left side of the arc with the abscissa. The Na and K films showed similar behavior.

The dependence of ionic conductivity on electrolyte content is shown in Figure 4. The appearance of a maximum ionic conductivity is similar to that observed in solutions of oligo(oxyethylene) dissolving $LiClO_4$, LiSCN, NaSCN, or KSCN.[13,29] An increase in salt concentration generally increases the number of carrier ions. However, the microviscosity of the conduction column is also increased, decreasing the mobility of carrier ions. The conductivity maxima in P(MEO_7–MALi) and P(MEO_7–MAK) are attributed to interaction of these two factors. An increase in cation radius increases the conductivity maximum and shifts it toward lower electrolyte content.

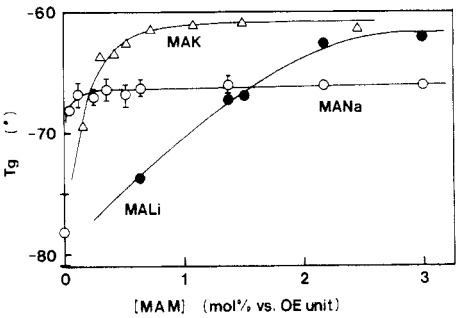

Figure 5. Relation between electrolyte content and T_g of P(MEO_7–MAM) films determined by DSC.

In the hybrid system P(MEO_7)/MSCN,[29] the conductivity of films containing large cations is higher than that with smaller ones because the dissociation energy of the added electrolytes in the films decreases with increasing cation radius. Furthermore, when a salt with lower dissociation energy is added to a polymeric solid electrolyte, the conductivity maximum should also be shifted to the lower salt content side. the conductivities of P(MEO_7–MALi) and P(MEO_7–MAK) are also strongly affected by the dissociation energy of added electrolytes on the low electrolyte content side. P(MEO_7–MANa) had lower conductivity, possibly because of the different chemical environment of the ions.

In order to clarify the relationship between ionic conductivity and segmental motion of the polymer matrix, the dependence of T_g on electrolyte content was determined (Figure 5). P(MEO_7–MALi) and P(MEO_7–MAK) show a clear relationship between MALi or MAK content and T_g at electrolyte contents below 2.4 and 0.7 mol %, respectively, whereas T_g became constant at higher electrolyte contents. The electrostatic interaction between cation and anion was stronger than the ion–dipole interaction between polymer and cation at these higher electrolyte contents. The large slope at low electrolyte content in P(MEO_7–MAK) is attributed to its higher dissociation than P(MEO_7–MALi). There are two factors involved in the increase of T_g with electrolyte content: (1) interaction between ether oxygen atoms and the cation increases the microviscosity of the film and (2) the polymer segment is expanded by the introduction of charges on the polymer backbone because of electrostatic repulsion. Poly(lithium methacrylate) has a T_g of around 130 °C, almost the same as those of the Na and K salts. If the increase in the T_g of P(MEO_7–MALi) and P(MEO_7–MAK) is caused by the second factor, their two curves (Figure 5) should have the same profile. That they do not suggests that the increase in T_g is caused by the first factor. The T_g calculated as a function of copolymer composition by the equations of Fox[30] and of Gordon and Taylor[31] was lower than the actual T_g for the P(MEO_7–MAM) polymers, supporting our conclusion that the first factor is primarily involved. On the other hand, P(MEO_7–MANa) has constant T_g at –67 °C when the sodium methacrylate content is increased beyond 0.2 mol %, the increase in electrolyte content being confirmed by IR. This result cannot be explained by the above two factors, and it is difficult to believe that MEO_7 and MANa were copolymerized homogeneously and the

Table I
WLF Parameters for P(MEO_7–MAM) Films

sample	(mol %)	T_g, °C	$\sigma(T_g)$, S/cm	C_1	C_2, deg	f_g	α_f, 10^{-4} deg^{-1}
MALi	(1.38)	−67.7	1.47×10^{-12}	8.38	65.3	0.052	7.9
MANa	(0.65)	−67.0	1.03×10^{-11}	6.55	92.1	0.066	7.2
MANa	(1.38)	−66.0	3.14×10^{-13}	8.54	66.6	0.051	8.6
MAK	(0.53)	−62.1	1.21×10^{-10}	5.99	85.4	0.073	8.5
WLF eq				17.4	51.6	0.025	4.8

MANa dissociated into ions.

Polarized optical micrographs of P(MEO_7–MANa) film (electrolyte content 1 mol %) showed blue, islandlike phase separation against a pink background, which remained after 90° rotation of the polarization plane. A similar effect was found in MANa powder and P(MANa). On the other hand, only the pink background was observed in P(MEO_7–MALi) and P(MEO_7–MAK) films at the same electrolyte content. These results suggest that the latter are fully amorphous in the electrolyte content range 0.1–0.4 mol %. The amorphous state was confirmed by DSC and X-ray diffraction measurements. However, two X-ray diffraction peaks were found in P(MEO_7–MANa) films containing >0.5 mol % Na^+. The broad peak at 2θ = 10–30° probably corresponds to the homogeneously copolymerized part of P(MEO_7–MANa) because this peak was also found in P(MEO_7–MALi) and P(MEO_7–MAK) films but not in P(MEO_7) film, P(MANa), or MANa. The sharp peak at 2θ = 32° may reflect MANa with a diffraction peak at the same scattering angle. Thus X-ray diffraction also supports phase separation in P(MEO_7–MANa).

The presence of low molecular weight electrolyte in the polymeric solid electrolyte might cause anionic conduction because both mobile cation and anion are generated by the dissociation of monomeric electrolyte, giving a bi-ion conductor. Generally, bi-ion conductors have much higher conductivities than single-ion conductors,[14] and the conductivity depends on the dissociation energy of the added salt. Thus added salts increase the conductivity of films in the order K > Na > Li.[29] The conductivity of P(MEO_7)/sodium butyrate is higher than those of P(MEO_7–MANa) and the hybrid system P(MEO_7)/lithium isobutyrate.[32] If the P(MEO_7–MANa) film was a hybrid bi-ion conductor, its conductivity should be higher than that of P(MEO_7)/sodium isobutyrate because methacrylate anion has a π-conjugated structure that reduces dissociation energy. However, the conductivity of P(MEO_7–MANa) is much lower than that of a hybrid bi-ion conductor (10^{-7} S/cm), suggesting that the anion and cation generated by dissociation of MANa contribute little to the ionic conductivity of P(MEO_7–MANa). However, the retention of luster in the film between Li electrodes indicates no proton conduction, and it appears that Na^+ is the sole carrier ion.

The temperature dependence of the ionic conductivity of P(MEO_7–MAM) films over the range 0–80 °C is shown in Figure 6. The curvature in the plots indicates that the ionic conduction obeys the Williams–Landel–Ferry (WLF) mechanism.[33] The WLF equation (eq 2) was used to

$$\log \frac{\sigma(T)}{\sigma(T_g)} = \frac{C_1(T - T_g)}{C_2 + (T - T_g)} \tag{2}$$

calculate the WLF parameters for log σ_i at different temperatures, where T = temperature (K), T_g = glass transition temperature (K), $\sigma(T)$ = conductivity at T (K), $\sigma(T_g)$ = conductivity at T_g, and C_1 and C_2 are WLF parameters. Since $\sigma(T_g)$ of the films was too small for us to measure, it was calculated by extrapolation to make the correlation

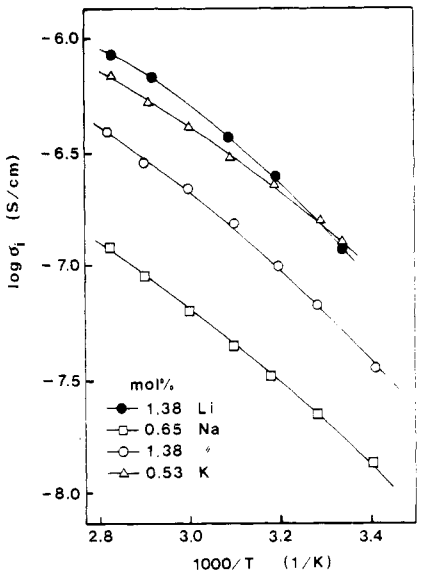

Figure 6. Temperature dependence of the ac (1 V) ionic conductivity in P(MEO_7–MAM) films.

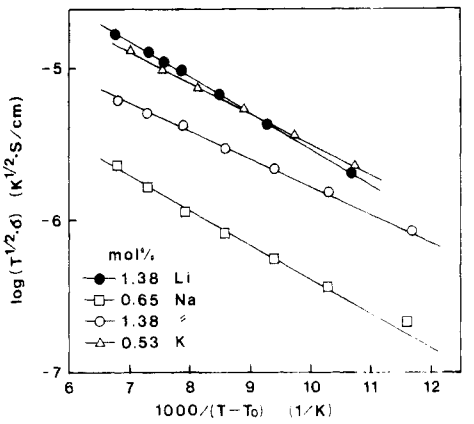

Figure 7. Vogel–Tammann–Fulcher plot of P(MEO_7–MAM) films.

between $(T - T_g)^{-1}$ and log $[\sigma(T)/\sigma(T_g)]$ linear by best-fit treatment with a computer. The calculated WLF parameters are shown in Table I; f_g, the free volume function at T_g, and α_f, the coefficient of thermal expansion, were calculated by $f_g = 1/2.303C_1$ and $\alpha_f = 1/2.303C_1C_2$ and are comparable to the WLF empirical values (C_1 = 17.4, C_2 = 51.6°). Thus the ionic conduction in P(MEO_7–MAM) is considerably affected by the segmental motion of polymer chains. This result also suggests that ionic conduction in P(MEO_7–MANa) occurs in the amorphous phase of the film.

The empirical Vogel–Tammann–Fulcher relation (eq 3) describes transport properties in a viscous matrix:[34]

$$\sigma = AT^{-1/2} \exp\left[\frac{-B}{(T - T_0)}\right] \tag{3}$$

where T = temperature (K), A and B = empirical constants, and T_0 corresponds to T_g.

If the ionic conduction of P(MEO_7–MAM) follows the WLF equation, the relationships between log ($\sigma T^{1/2}$) and $(T - T_0)^{-1}$ should be linear, as they are in Figure 7.

Conclusion

Polymeric solid electrolytes with single-ion conductor properties were prepared by copolymerization of oligo(oxyethylene) methacrylate and alkali-metal methacrylates. A dc ionic conductivity of 10^{-6} S/cm at 80 °C for Li ions was stable over time. The conductivities of these films depend mainly on the chemical environment of the ions in the polymer matrix. The temperature dependence of the ionic conductivity suggests that the conduction follows the WLF mechanism, which is confirmed by determination of WLF parameters and by Vogel–Tammann–Fulcher plots. Thus the single-ion conductivity of these polymeric electrolytes is strongly affected by segmental motion in the polymer matrix.

Acknowledgment. This work was partially supported by a Grant-in-Aid for Scientific Researches from the Ministry of Education, Science and Culture, Japan.

Registry No. (MEO_7)(MANa) (copolymer), 111349-67-8; (MEO_7)(MALi) (copolymer), 111349-68-9; (MEO_7)(MAK) (copolymer), 111349-69-0.

References and Notes

(1) Tsuchida, E.; Ohno, H.; Tsunemi, K. *Electrochim. Acta* **1983**, *28*, 591, 833.
(2) Tsuchida, E.; Ohno, H.; Tsunemi, K.; Kobayashi, N. *Solid State Ionics* **1983**, *11*, 227.
(3) Shigehara, K.; Kobayashi, N.; Tsuchida, E. *Solid State Ionics* **1984**, *14*, 85.
(4) Wright, P. V. *Br. Polym. J.* **1975**, *319*, 137.
(5) Papke, B. L.; Ratner, M. A.; Shriver, D. F. *J. Phys. Chem. Solids* **1981**, *42*, 493.
(6) Berthier, C.; Gorecki, W.; Minier, M.; Armand, M. B.; Chabagno, J. M.; Riguad, P. *Solid State Ionics* **1983**, *11*, 91.
(7) Dupon, R.; Papke, B. L.; Ratner, M. A.; Whitmore, D. H.; Shriver, D. F. *J. Am. Chem. Soc.* **1982**, *104*, 6247.
(8) Weston, J. E.; Steel, B. C. H. *Solid State Ionics* **1982**, *7*, 81.
(9) Killes, A.; Le Nest, J. F.; Gandini, A.; Cheradame, H. *Macromoleculs* **1984**, *17*, 63.
(10) Watanabe, M.; Ikeda, J.; Shinohara, I. *Polym. J.* **1983**, *15*, 65, 175.
(11) Watanabe, M.; Sanui, K.; Ogata, N.; Kobayashi, T.; Ohtaki, Z. *J. Appl. Phys.* **1985**, *57*, 123.
(12) Yang, L. L.; McGhie, A. R.; Farrington, G. C. *J. Electrochem. Soc.* **1986**, *133*, 1380.
(13) Kobayashi, N.; Uchiyama, M.; Shigehara, K.; Tsuchida, E. *J. Phys. Chem.* **1985**, *89*, 987.
(14) Kobayashi, N.; Uchiyama, M.; Tsuchida, E. *Solid State Ionics* **1985**, *17*, 307.
(15) Kobayashi, N.; Hamada, T.; Ohno, H.; Tsuchida, E. *Polym. J.* **1986**, *18*, 661.
(16) Watanabe, M.; Rikukawa, M.; Sanui, K.; Ogata, N.; Kato, H.; Kobayashi, T.; Ohtaki, Z. *Macromolecules* **1984**, *17*, 2902.
(17) Dupon, R.; Papke, B. L.; Ratner, M. A.; Shriver, D. F. *J. Electrochem. Soc.* **1984**, *131*, 586.
(18) Chiang, C. K.; Davis, G. T.; Harding, C. A.; Takahashi, T. *Macromolecules* **1985**, *18*, 825.
(19) Clancy, S.; Shriver, D. F.; Ochrynowycz, L. A. *Macromolecules* **1986**, *19*, 606.
(20) Blonsky, P. M.; Shriver, D. F.; Austin, P.; Allcock, H. R. *J. Am. Chem. Soc.* **1984**, *106*, 6854.
(21) Bannister, D. J.; Davies, G. R.; Word, I. M.; McIntyre, J. E. *Polymer* **1984**, *25*, 1600.
(22) Xia, D. W.; Soltz, D.; Smid, J. *Solid State Ionics* **1984**, *14*, 85.
(23) Le Mehaute, A.; Crepy, G.; Marcellin, G.; Hamaide, T.; Guyot, A. *Polym. Bull.* **1985**, *14*, 233.
(24) Bannister, D. J.; Davies, G. R.; Word, I. M.; McIntyre, J. E. *Polymer* **1984**, *25*, 1291.
(25) Hardy, L. C.; Shriver, D. F. *J. Am. Chem. Soc.* **1985**, *107*, 3823.
(26) In methacrylic acid, $\nu_{C=O}$ was observed at 1695 cm^{-1}, whereas in alkali-metal methacrylates $\nu_{C=O}$ appeared at 1560 cm^{-1}. Therefore no signal at 1695 cm^{-1} indicated the pure MAM structure.
(27) Cole, K. S.; Cole, R. H. *J. Chem. Phys.* **1941**, *9*, 341.
(28) Watanabe, M.; Rikukawa, M.; Sanui, K.; Ogata, N. *J. Appl. Phys.* **1985**, *58*, 736.
(29) Kobayashi, N.; Ohno, H.; Tsuchida, E. *J. Chem. Soc. Jpn.* **1986**, 441.
(30) Fox, T. G.; *Bull. Am. Phys. Soc.* **1956**, *1*, 123.
(31) Gordon, M.; Taylor, J. S. *J. Appl. Chem.* **1952**, *2*, 493.
(32) Reference acid salt [$CH_3CH(CH_3)COOLi$] for methacrylate salt [$CH_2{=}C(CH_3)COOLi$].
(33) Williams, M. L.; Landel, R. F.; Ferry, J. D. *J. Am. Chem. Soc.* **1955**, *77*, 3701.
(34) (a) Vogel, H. *Phys. Z.* **1921**, *22*, 645. (b) Tammann, V. G.; Hesse, W. Z. *Anorg. Allg. Chem.* **1926**, *156*, 245. (c) Fulcher, G. C. *J. Am. Ceram. Soc.* **1925**, *8*, 339.